Asia-Pacific Journal of Science and Technology: Volume: 29. Issue: 01. Article ID.: APST-29-01-10. Research Article

APST

Asia-Pacific Journal of Science and Technology

https://www.tci-thaijo.org/index.php/APST/index

Published by the Research and Graduate Studies,
Khon Kaen University, Thailand

Rice cropping systems classification using time-series Landsat images and Phenology-based algorithms in Suphan Buri, Thailand

Chattida Singkawat[1,2] and Kritchayan Intarat[1,*]

[1]Department of Geography, Faculty of Liberal Arts, Thammasat University, Pathum Thani, Thailand
[2]Infraplus Co., Ltd., Bangkok, Thailand
[*]Corresponding author: intaratt@tu.ac.th

Received 1 September 2022
Revised 20 November 2022
Accepted 2 January 2023

Abstract

Suphan Buri, a province in the central region of Thailand, is essentially a rice producing and exporting area of Thailand. This study aims to classify rice cropping systems, applying a phenological and pixel-based paddy rice mapping (PPPM) algorithm along with the cutting-edge Google Earth Engine (GEE) cloud platform. Four cropping systems i.e., single rice crop (SCR), double rice crop (DCR), two and a half rice crop (THCR), and triple rice crop (TCR), are duly investigated. To support agricultural policies and irrigation, rice cropping systems can provide vital information. Such an approach can analyze the heading-period rice's phenology using the Enhanced Vegetation Index (EVI) retrieved from the Landsat 8 time-series images. Statistical assessments are employed to evaluate the rice cropping systems, revealing the high performance of the PPPM model. Overall results are seen to be highly successful, attaining an accuracy of 0.91; Kappa statistics reach 0.80. GEE reveals many advantages in geospatial analysis.

Keywords: Rice phenology, Remote sensing, Time-series analysis, Rice cropping systems, Google Earth Engine

1. Introduction

The major meal for half of global inhabitants is cultivated in Asia (over 90% of rice). In Southeast Asia, Thailand is among the top three rice exporting countries [1]. Due to the flood plain terrain, the central region of Thailand contains many irrigated systems that benefit the rice cropping system. Double cropping rice is mainly found in such an irrigated area. Five or six crops of rice can be planted every two years where potential irrigation is presented. Nowadays, climate variability impacts most agricultural plantations, resulting in the vulnerability of rice production [2]. It is noted that some irrigated areas cannot deliver sufficient water causing the reduction of rice cropping. Thus, acquiring a rice cropping system in the region can benefit agricultural policy and water management [3]. The spatiotemporal variation of the multiple rice cropping system is one of the most crucial pieces of information to support rice cultivation. Accurate estimating of these changes is essential, and such information can support local agricultural policies and ensure effective irrigation operations.

In a large area of rice cropping systems, remotely sensed data has, therefore, been introduced. This platform can provide timely and precise information on rice cultivation, gathering observations of the earth's surface and analyzing various data [4,5]. Previous reports have revealed the utilization of remotely sensed data for determining the stages of growing rice [6,7]. Products from Moderate Resolution Imaging Spectroradiometer (MODIS) have long been associated with this task and have demonstrated adequate results; due to poor spatial resolution (250 – 500 m resolution), sub-pixel homogeneity is seen as a drawback [8,9]. Detection of rice cropping systems in moderate areas has been enhanced by incorporating higher spatial resolution products such as Landsat (30 m) [3,10] and Sentinel (10-60 m) [5,6], thus revealing greater improvement in accuracy.

Several studies have indicated the ability of time-series remote sensing applications for delineating rice cropping systems using crop phenological information. Some filtering techniques have also been examined to reduce the noise from cloud effects, atmospheric variables, and satellite sensors' discrepancies [11]. Such approaches have been recommended viz. Wavelet Transforms [12], Savitzky–Golay (SG) [13], Empirical Mode

Decomposition (EMD) [14], and the Harmonic Model [3]. Because of its flexibility, the Harmonic Model, based on Fourier transform, is preferable in remote sensing applications [15]. The Harmonic Model can account for cyclicality with simple or reproduced shapes. Furthermore, the ordered nature of the cosine curve can also approximate the data's seasonal trend. This technique can reduce discrepancies from the vegetation index time-series. For example, an Enhanced Vegetation Index (EVI), designed to improve the vegetation signal, can quantify the greenness of vegetation and be more responsive to canopy variations [16]. EVI is seen to be compatible with the Harmonic Model, which can analyze a complex curve to the sum of cosine wave (terms) as well as an additive term series [17,18].

In the rice cropping systems, three methods are employed: machine learning [9], statistical approaches [10], and a phenology and pixel-based paddy rice mapping (PPPM) algorithm [3]. Machine learning requires fitting training patterns due to long-term classification [19]. Statistical approaches rely on data quantity where key phenology is not considered. In contrast, PPPM can efficiently settle rice growth stages by incorporating rice's phenology. The PPPM algorithm has been carried out in previous works and has proved to be successful in identifying rice cropping systems. This approach is preferable when associated with the time-series dataset and a large experimental area. The use of PPPM can deliver more than 85% accuracy on rice cropping detection and can reduce computation time [20]; The phenology derived from vegetation indices can indicate the rice-growing stage correctly. Zhu et al. [3] successfully employed the PPPM algorithm, associating the first derivative for detecting the rice's vegetation index profile in the heading period. Such a method has been used to analyze the long-period dynamic based on time-series phenology in China [20]. PPPM can achieve high accuracy along with kappa testing of double-cropping rice classification.

Dealing with data series, especially remotely sensed data, is quite challenging. Recently, Google Earth Engine (GEE), a cutting-edge platform, has been introduced and has played a key role in the analysis of geospatial big data. For over 40 years, GEE has been freely accessible and has provided large datasets such as satellite imagery and other geospatial data collections [21]. Such a lengthy period of data helps to better improve time-series studies. GEE is also seen to ensure satisfactory operation in rice cropping discrimination by supporting vast information and computing resources [22,23].

To the best of our knowledge, regarding the rice cropping system in Thailand, previous classification merely identified single and double rice crops [24]. Through better management, however, of irrigation, multiple rice crops have been improved, encompassing single, double, two and a half, and triple crops. Herein, this paper sets out to classify the systems of rice cropping by incorporating the cutting-edge GEE platform with rice phenological data. To monitor the systems of rice cropping, the PPPM algorithm was duly applied [3,8]. Thus, acquisition of data was extended from one year to two years to find the optimum time-series satellite images and the local threshold for indicating the four types of crop rice. Suphan Buri Province was selected as the experimental area. In this region, Thai rice benefits from continual rainfall and its extensive irrigation system. In Nong Ya Sai and Don Chedi District, only single crop rice is cultivated. In the fertile irrigated zone of Suphan Buri, multiple rice crops flourish. Suphan Buri was found to be appropriate for classifying the rice cropping systems.

2. Materials and methods

2.1 Study area

The selected study site is Suphan Buri Province, Thailand, with coordinates N 14°30′49.69″ and E 100°07′50″ (Figure 1). The province is approximately 10 meters high above the mean sea level, with a slight slope from the western to the southeastern region. Cultivation of rice covers on area of 2,400 sq km. Most rice fields are located in the eastern part where the Tha Chin River (Suphan Buri river) courses through the area. In May to June, the single-crop rice starts and is harvested from August to September. The cultivation of double cropping starts in October and is harvested around January to February. Triple-cropping begins in February and is finished during April to May [24].

2.2 Data

2.2.1 Landsat 8 time-series selection

In this experiment, Landsat 8 imageries were acquired via the GEE cloud product LANDSAT/LC08/C02/T1_TOA with a 30-m resolution and 16-days revisiting time. Three scenes of imageries were merged to cover the experimental area using path/row 129/50, 130/49, and 130/50, respectively. This collection-2 and tier-1 Landsat 8 images provided the top of atmospheric (TOA) reflectance. Many products were improved viz. geometric accuracy, radiometric calibration, digital elevation modeling, and quality assessment e.g., QA_PIXEL. The tier-1 Landsat 8 data was also recommended for its association with multi-temporal and pixel-based analysis [25]. Landsat 8’s precision and terrain has already been corrected using ground control points

(GCPs) and the digital elevation model (DEM) for further radiometric calibration and atmospheric correction [26]. The experiment was carried out between April 1, 2020, and March 31, 2022. It is noted that two years of multi-temporal images were acquired to determine the phenological stages of rice, generating 2.5 rice crop cycles.

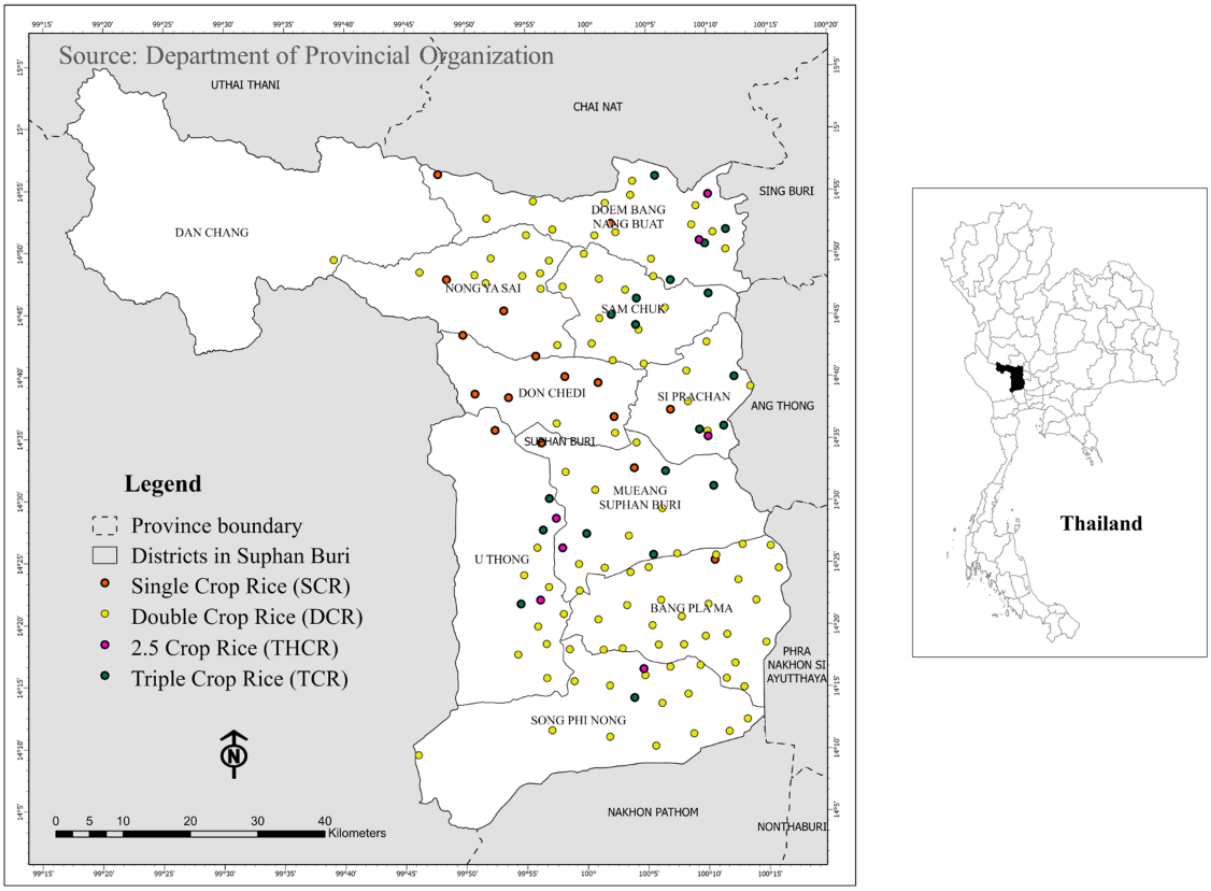

Figure 1 Schema of the Suphan Buri Province: the major rice cultivation zone in the central flood plain region. The orange, yellow, magenta, and blue dots correspond to the single, double, two and a half, and triple crop rice, respectively.

2.2.2 Secondary data and field survey

Both the Suphan Buri boundary and irrigation zone were utilized to specify the experimental location. The non-rice crop was determined and masked using the land-use map obtained from the Land Development Department (LDD) [27]; thereby, leveraging the rice cropping system detection's accuracy. Field observation was performed in all districts of rice cultivation. For assessment of accuracy, rice's biological data and cropping number per year were gathered from 140 checkpoints.

2.3 Methodology

The experimental method focused on four main steps: 1) Removing the time-series bad observations from the Landsat 8 image using TOA 2) Calculating the vegetation index from the multiple images to witness rice phenology 3) Utilizing the Harmonic Model and first derivative to detect rice's heading stage, and 4) The confusion matrix was applied for accuracy assessment. In Figure 2, all processes are presented.

2.3.1 Removing bad observations

All Landsat 8 time-series images were acquired via the GEE cloud platform during the selected period. According to TOA reflectance, effects from clouds, atmospheric aerosols, and gases were contaminated [28]. Hence, the pixel quality assessment band (from "LANDSAT/LC08/C02/T1_TOA" collection) was then utilized to identify the bad observations. The QA Bitmask (known as QA_PIXEL band) was seen to be beneficial in

specifying each pixel that revealed bad observations less than 0.8 such that it could be analyzed by the Harmonic Model [29].

2.3.2 Calculation of vegetation index

Initially, the PPPM algorithm applied the correlation between the Enhance Vegetation Index (EVI)/ Normalized Difference Vegetation Index (NDVI) and Land Surface Water Index (LSWI) for detecting paddy rice that is grown in a mixture of water and soil [8]. In this experiment, non-rice crops were masked, making the Land Surface Water Index (LSWI) unnecessary for assessment of the cropping systems. Due to its atmospheric correction and improvement of canopy background signals, EVI was selected [30]. It is observed that EVI is sensitive to canopy types and dense vegetation areas, and can be expressed as follows:

$$\mathrm{EVI} = \mathrm{G}\frac{(\mathrm{NIR} - \mathrm{RED})}{(\mathrm{NIR} + \mathrm{C1} \times \mathrm{RED} - \mathrm{C2} \times \mathrm{BLUE} + \mathrm{L})} \quad (1)$$

where NIR is near-infrared, RED is visible red, BLUE is visible blue, G is gaining factor, C1 and C2 are coefficients for atmospheric resistance, L is the value obtained to adjust the background of the canopy. The coefficient' values used in the Landat-8 images depend on MODIS-EVI algorithms: L=1, C1 = 6, C2 = 7.5, and G = 2.5, respectively.

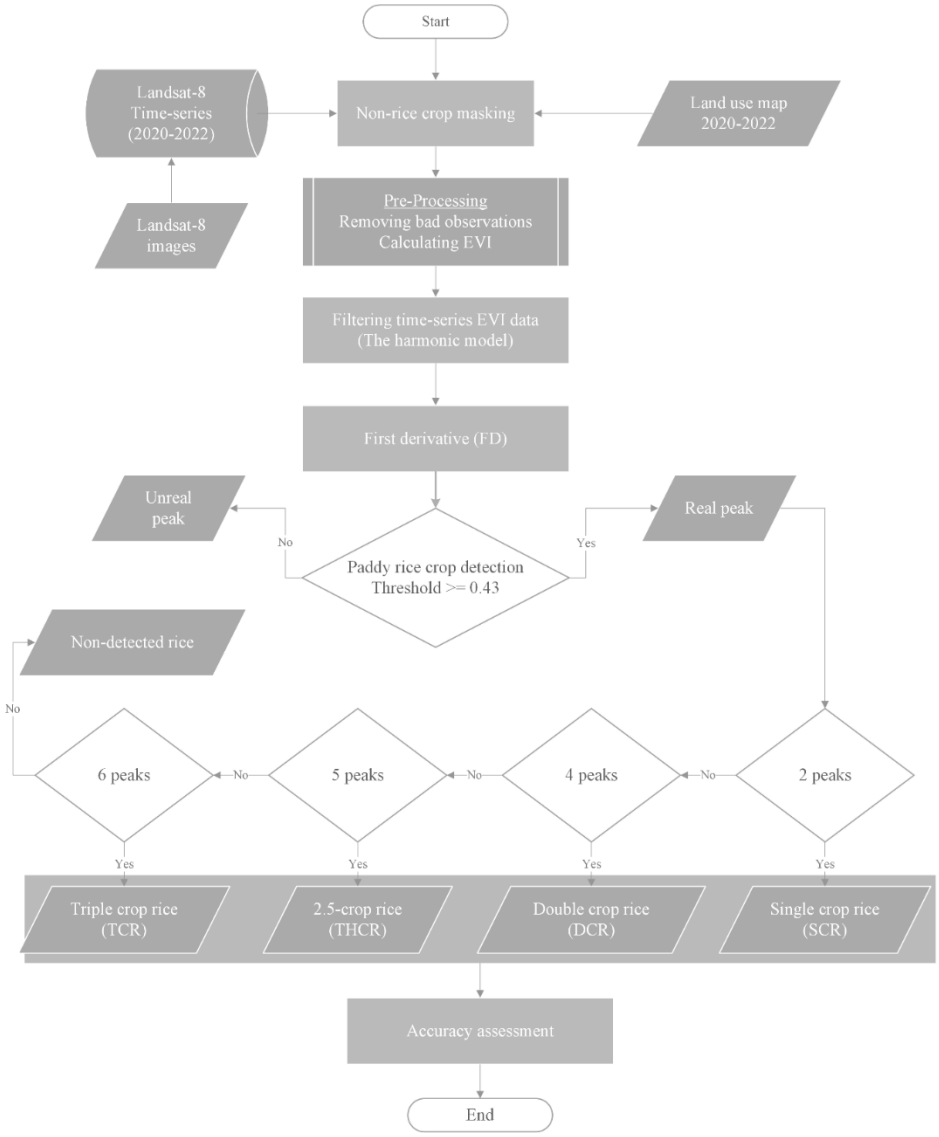

Figure 2 Flowchart of the methodology.

2.3.3 Detection of rice's heading stage

To avoid insufficient information, detailed EVI observations were acquired over two years. Due to the cloud issue, the Harmonic Model was applied to the entire collection. The Harmonic Model is able to compute both amplitude and angles of the phases, establishing complex curves through the order of cosine waves, thereby transforming weak signals into high-quality signals, as revealed in Equation (2). Thus, the smoothed-EVI revealed the time-series peaks, which is the key phenology to detect rice's heading period and classify the rice's cropping system (Figure 3). The more observations of EVI images, the more accurate the noise filtering:

$$Pt = \beta_0 + \beta_1 t + \beta_2 \cos(2\pi\omega t) + \beta_3 \sin(2\pi\omega t) + e_t \quad (2)$$

where Pt is the pixel's value after using the harmonic model, β_0 and β_1 are the linear regression coefficients, $\beta_2 = A\cos(\varphi)$, $\beta_3 = A\sin(\varphi)$, $A = (\beta_{2^2} + \beta_{3^2})$, ω is the frequency, t is the timestep, φ is the phase and e_t is a random error.

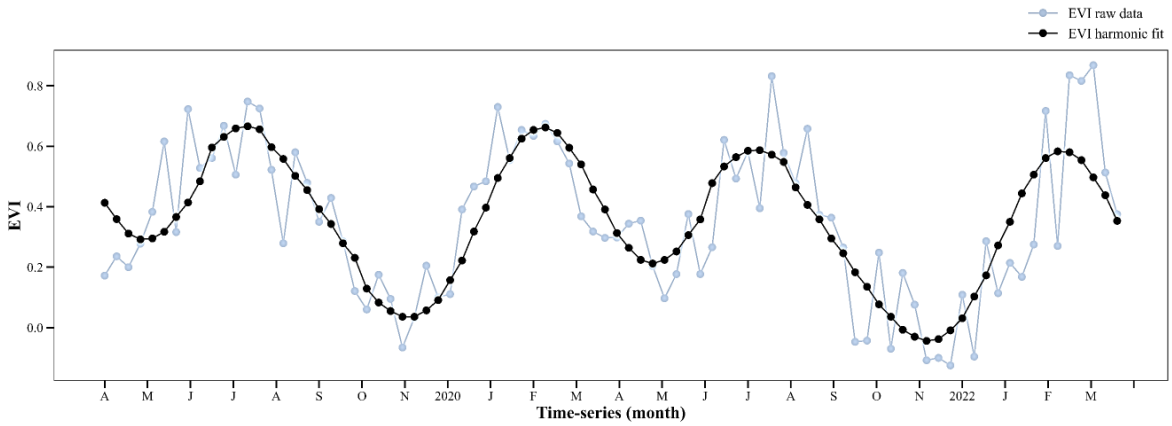

Figure 3 The smoothed-EVI plot using the Harmonic model. The light blue-dot line reveals the raw EVI and the black-dot line exhibits the improved EVI signal after fitting.

After the removal of noise from the EVI curve, the first derivative (FD analysis) proposed by Zhu et al. [3] was then applied to the EVI-smoothed curve for detection of rice's heading period. In the original FD analysis, the date's difference during a year (ΔDOY) was replaced by the date's difference from the time stamp of each image. The replacement allowed for multiple dates of the time-series data to be calculated and analyzed. Thus, the FD analysis can be expressed, as in Equation (3)

$$FD_{VI} = (EVI_{(j+i)} - EVI_{(j)})/\Delta \text{ system: time\_start} \quad (3)$$

where FD_{VI} is the FD value of EVI between the j^{th} and $j+1^{th}$ of image time stamp, EVI_j is the EVI value at the j^{th} of image time stamp, EVI_{j+i} is the EVI value at the $j+1^{th}$ of image time stamp, and Δ system: time start is the date difference from time stamp.

FD analysis was investigated through the smoothed-EVI time series from early to the later date: f'(x) > 0 means positive functions change (increasing functions), according to an increasing EVI rate. When f'(x) < 0 negative functions change (decreasing functions): the EVI rate declines from the local maxima. On the other hand, f'(x) = 0 affirms no function changed, indicating the local maxima point as the rice heading period or peak. This case also exhibited maximum EVI in the time-series collection.

Nonetheless, artificial peaks e.g., grassland can be detected, resulting in misclassification (Figure 4A). Xiao, et al. [8] speculated on this issue. Following the guidelines, the analysis obtained the EVI value of the actual rice pixel by gaining half of the maximum value in the rice cycle. By this means, the average value of maximum EVI through the time-series collection was able to be calculated. A threshold of 0.43 was extracted and applied to detect actual peaks; below-threshold peaks were eliminated from the detection.

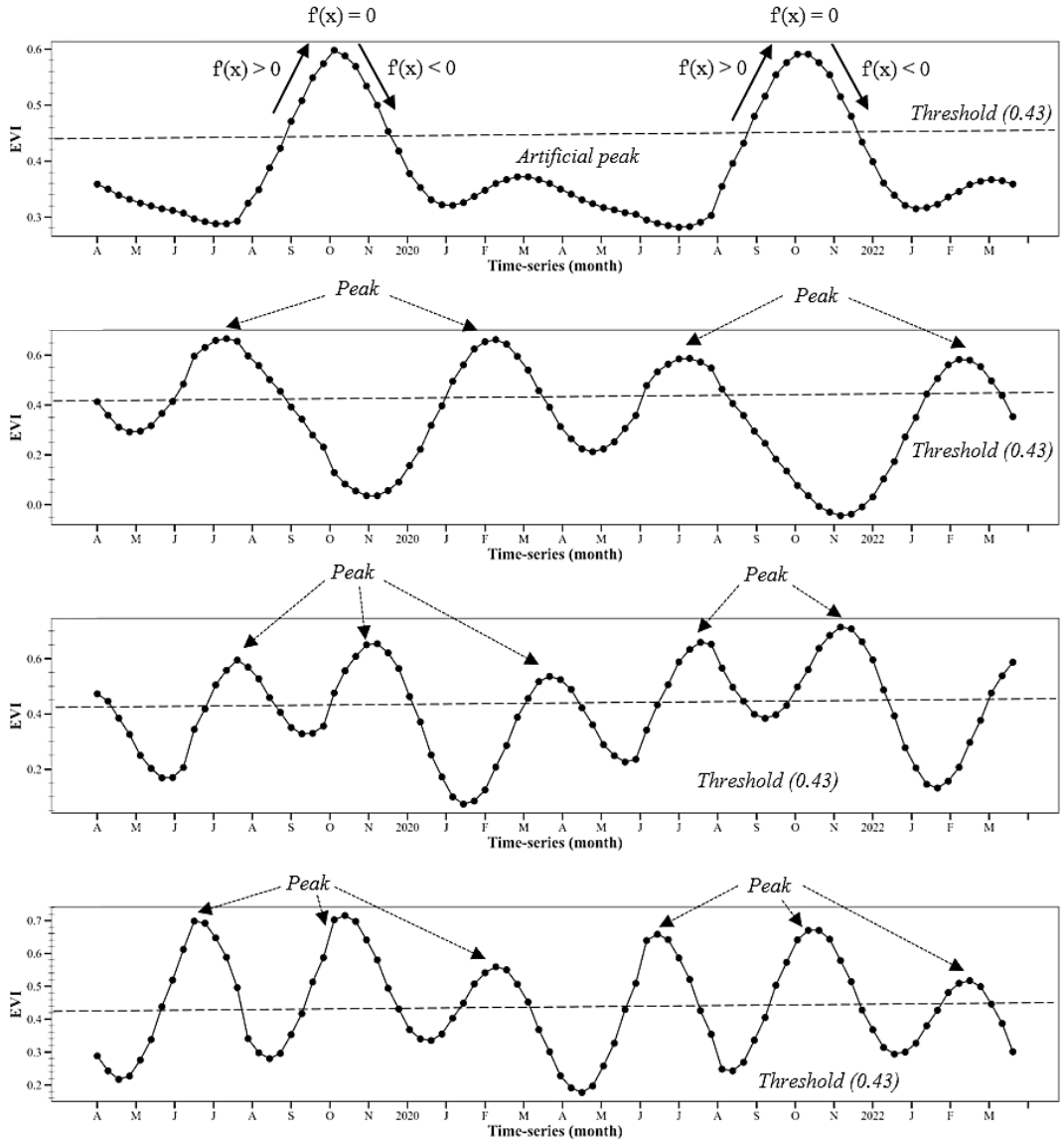

Figure 4 Fitted EVI of rice phenology, in which (A) = single cropping systems (1 crop per year), (B) = double cropping systems (2 crops per year), (C) = 2.5 crops per year, and (D) = triple cropping systems (3 crops per year).

3. Results

As obtained from the District Agricultural Extension Office, the rice cropping system map was compared with 140 ground-referenced data: single crop rice (SCR) = 16 points, double crop rice (DCR) = 98 points, two and a half crop rice (THCR) = 7 points, and triple crop rice (TCR) = 19 points, as displayed in Figure 1. Subsequently, the results were displayed in a confusion matrix, from which four accuracy metrics were calculated, overall accuracy (OA), producer's accuracy (PA), user's accuracy (UA), and kappa coefficient (Table 1). Overall accuracy and Kappa statistics proved to be 0.91 and 0.80, respectively.

Table 1 Classification accuracy assessment.

Ground reference data	Classification results				Total
	SCR	DCR	THCR	TCR	
SCR	13	3	0	0	16
DCR	1	94	3	0	98
THCR	0	3	4	0	7
TCR	1	0	2	16	19
Total	15	100	9	16	140
Producer accuracy	0.87	0.94	0.44	1.00	
User accuracy	0.81	0.96	0.57	0.84	
Overall accuracy	0.91				
Kappa statistics	0.80				

As reported in Table 1, the classification results correspond to the ground reference data. Double crop rice (DCR) is the primary rice cropping system in the investigation. Producer accuracy displayed a high classification result for three rice cropping systems e.g., 0.87, 0.94, and 1.00 for SCR, DCR, and TCR, respectively. Such high values are typical when three rice cropping systems are applied in the area. User accuracy again demonstrated the reliability of the classification of the rice cropping systems; SCR, DCR, and TCR indicated high reliability, attaining 0.81, 0.96, and 0.84, respectively. THCR evaluations for both producer and user accuracies i.e., 0.44 and 0.57 proved to be very low. The small area of THCR cultivation in the study area may cause the mixing of signals and can lead to the evaluation's discrepancy [19].

According to the classification in Figure 5, SCR was basically found in the western region of Suphan Buri Province e.g., Don Chedi and Nong Ya Sai Districts. These districts are located outside the irrigation zone. The other source of water supply was mainly obtained from groundwater. In this non-irrigation site, some DCR, THCR, and TCR were cultivated among the SCR [24]. In contrast, the eastern region of Suphan Buri Province possessed a vast irrigated zone (the boundary within the blue stripes in Figure 5). DCR, THCR, and TCR were distributed extensively throughout many districts e.g., Sam Chuck, Si Prachan, and Song Phi Nong. Water supply was also available from the Tha Chin River (blue-filled boundary in Figure 5), which could well support the multiple rice cropping. Furthermore, photoperiod intensive and short cycle (105 days of growing) rice varieties were also chosen to grow in this irrigated region. These additional factors, i.e., rice irrigation, rice varieties, groundwater and rivers are seen to be encouraging multiple rice cropping systems as well.

4. Discussion

This experiment utilized the PPPM algorithm to detect the rice cropping system in Suphan Buri Province. Rice cropping was divided into four classes: SCR, DCR, THCR, and TCR. Detection employed the first derivative to acquire the peak from the phenology of rice and proved to be flexible and consistent when applied to the various rice cropping. According to signal detection, signature quality is the critical factor in detecting the heading period. The Landsat satellite is repeated every 16 days at the exact location to counteract missing data from the cloud's discrepancy. This concern reveals the difficulty with the actual rice cropping system of detection using only one-year time-series information. The Harmonic Model applied in this experiment required sufficient satellite observations for corrective data filtering [3]. This experiment employed a two-year EVI to obtain the rice's time-series signal. The number of peaks in its crop system was counted twice, resulting in two peaks for SCR, four for DCR, five for THCR, and six for TCR, respectively.

It is acknowledged that the universal problem of optical satellite imagery applications is cloud coverage [20,31]. Cloud coverage has revealed the disadvantages of PPPM algorithms. The results can be confusing due to observation of artificial peaks. This discrepancy can influence empirical values; actual peaks cannot be detected. In other words, the Harmonic Model cannot fit the actual EVI, reflecting the false rice's phenology [23]. Such a drawback can lead to misidentification and uncertainty of the rice crop system, especially in the THCR class; the mixed cultivation e.g., sugarcane, cassava, and maize between rice and other crops anticipate such an outcome [24]. The threshold-based technique suggested by Son et al. [19] was associated with this experiment to avoid unrealistic peaks containing low EVI values. In contrast, some necessary peaks may be excluded; The threshold-based method sometimes determines the nearest threshold value as a false signal, reducing rice crop numbers.

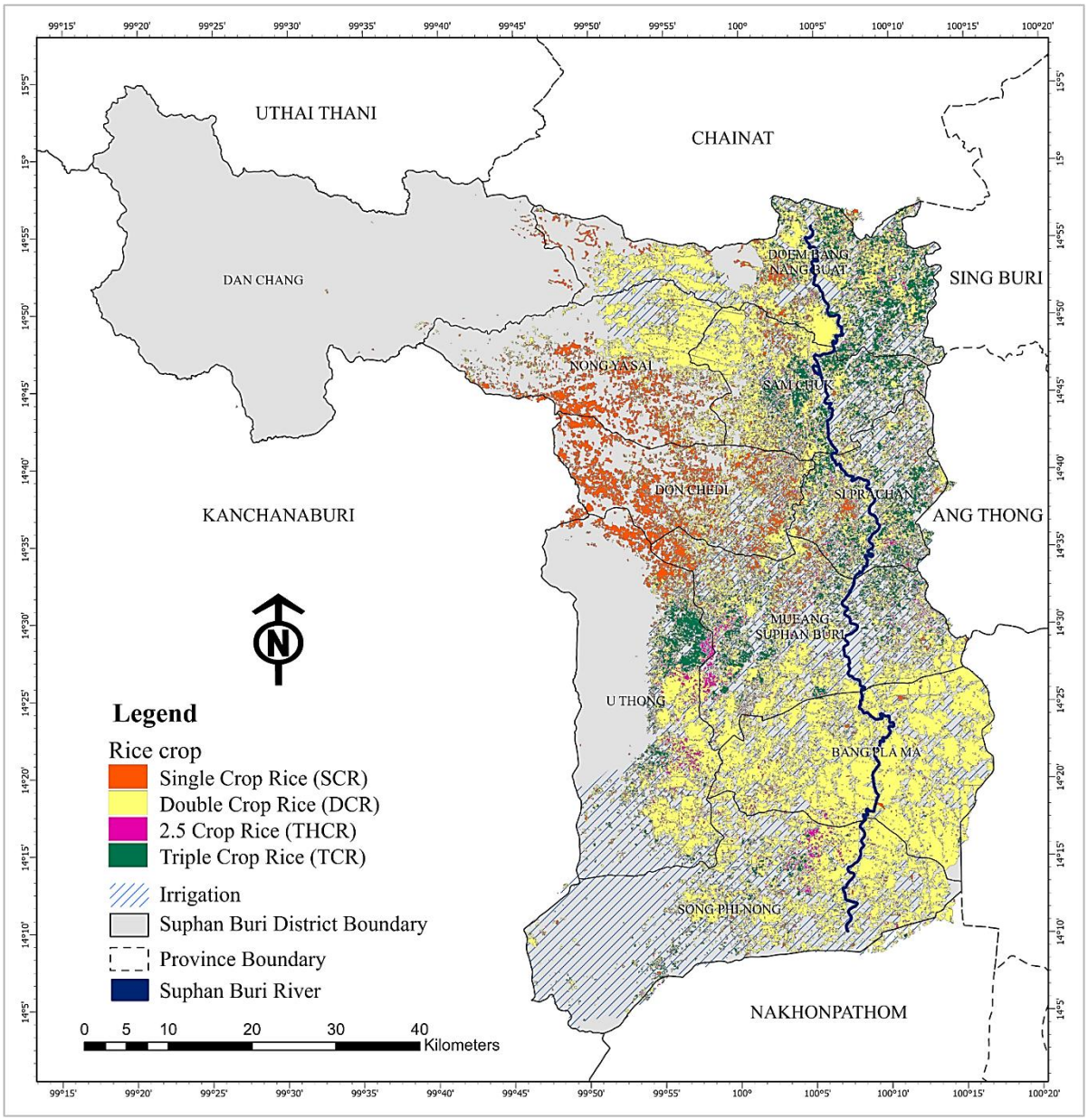

Figure 5 Classification map of the rice crop systems: the orange, yellow, magenta, and green boundaries reveal single, double, two-and-a-half, and triple-crop rice.

5. Conclusion

In this study, during 2020-2022, the EVI time-series investigated the classification of the rice cropping system in Suphan Buri Province. To extract the number of rice peaks, the developed PPPM algorithm was applied to two-year time-series Landsat 8 imageries. This methodology revealed a high performance, attaining 0.91 classification accuracy. Moreover, the application of the GEE platform demonstrated high potential for processing both time-series information, acquired from satellite imagery, and classification of rice cropping over a large area. Such information can benefit local authorities in the management of irrigation. Besides, classified rice cropping can support other policies e.g., crop insurance and preparedness of natural hazards. The method used in this study can also be applied or adapted to other rice cultivation areas using the GEE cloud computing platform.

6. Acknowledgments

We would like to express our gratitude to The Rice Department and District Agricultural Extension Office, Suphan Buri Province, for the kind support of validation data to complete this study. Our thanks also extend to the Thailand Rice Science Institute (TRSI) for supporting our field trip in Suphan Buri Province.

7. References

[1] A Arunmas P. 2022 rice exports to reach 7.5m tonnes [Internet]. 2021 [cited 2022 May 4]. Available from: https://www.bangkokpost.com/business/2231983/2022-rice-exports-to-reach-7-5m-tonnes.

[2] Somboonsuke B, Phitthayaphinant P, Sdoodee S, Kongmanee C. Farmers' perceptions of impacts of climate variability on agriculture and adaptation strategies in Songkhla Lake basin. Kasetsart J Soc Sci. 2018;39(2):277-283.

[3] Zhu L, Liu X, Wu L, Liu M, Lin Y, Meng Y, et al. Detection of paddy rice cropping systems in southern China with time series Landsat images and phenology-based algorithms. GIScience Remote Sens. 2021;58(5):733-755.

[4] Guan X, Huang C, Liu G, Meng X, Liu Q. Mapping rice cropping systems in Vietnam using an NDVI-based time-series similarity measurement based on DTW distance. Remote Sens. 2016;8(1):19.

[5] Zhao R, Li Y, Ma M. Mapping paddy rice with satellite remote sensing: a review. Sustainability. 2021;13(2):503.

[6] Ramadhani F, Pullanagari R, Kereszturi G, Procter J. Automatic mapping of rice growth stages using the integration of sentinel-2, mod13q1, and sentinel-1. Remote Sens. 2020;12(21):3613.

[7] Xu L, Zhang H, Wang C, Wei S, Zhang B, Wu F, et al. Paddy rice mapping in thailand using time-series sentinel-1 data and deep learning model. Remote Sens. 2021;13(19):3994.

[8] Xiao X, Boles S, Liu J, Zhuang D, Frolking S, Li C, et al. Mapping paddy rice agriculture in southern China using multi-temporal MODIS images. Remote Sens Environ. 2005;95(4):480-492.

[9] Chen CF, Chen CR, Son NT. Investigating rice cropping practices and growing areas from MODIS data using empirical mode decomposition and support vector machines. GIScience Remote Sens. 2012;49(1):117-138.

[10] Chen Y, Lu D, Luo L, Pokhrel Y, Deb K, Huang J, et al. Detecting irrigation extent, frequency, and timing in a heterogeneous arid agricultural region using MODIS time series, Landsat imagery, and ancillary data. Remote Sens Environ. 2018;204:197-211.

[11] Amri SS, Kalyankar NV, Khamitkar SD. A comparative study of removal noise from remote sensing image. arXiv. 2010;preprint arXiv:10021148.

[12] Chen CF, Son NT, Chen CR, Chang LY. Wavelet filtering of time-series moderate resolution imaging spectroradiometer data for rice crop mapping using support vector machines and maximum likelihood classifier. J Appl Remote Sens. 2011;5(1):053525.

[13] Guan X, Huang C, Liu G, Meng X, Liu Q. Mapping rice cropping system in Vietnam using an NDVI-based time-series similarity measurement based on DTW distance. Remote Sens. 2016;8(19):1-25.

[14] Chen CF, Son N, Chang L, Chen C. Classification of rice cropping systems by empirical mode decomposition and linear mixture model for time-series MODIS 250 m NDVI data in the Mekong Delta, Vietnam. Int J Remote Sens. 2011;32(18):5115-34.

[15] Deijns AA, Bevington AR, Zadelhoff F, Jong SM, Geertsema M, McDougall S. Semi-automated detection of landslide timing using harmonic modelling of satellite imagery, Buckinghorse river, Canada. Int J Appl Earth Obs Geoinf. 2020;84:101943.

[16] Somvanshi SS, Kumari M. Comparative analysis of different vegetation indices with respect to atmospheric particulate pollution using sentinel data. Appl Comput Geosci. 2020;7:100032.

[17] Jakubauskas ME, Legates DR, Kastens JH. Harmonic analysis of time-series AVHRR NDVI data. Photogramm Eng Remote Sensing. 2001;67(4):461-70.

[18] Ghidora77. Time Series Modeling [Internet]. 2022 [cited 2022 May 1]. Available from: https://developers.google.com/earth-engine/tutorials/community/time-series-modeling.

[19] Son NT, Chen CF, Chen CR, Duc HN, Chang LY. A phenology-based classification of time-series MODIS data for rice crop monitoring in Mekong Delta, Viet Remote Sens. 2013;6(1):135-156.

[20] Zhao R, Li Y, Ma M. Mapping paddy rice with satellite remote sensing: a review. Sustainability. 2021;13(2):503.

[21] Tamiminia H, Salehi B, Mahdianpari M, Quackenbush L, Adeli S, Brisco B. Google earth engine for geo-big data applications: a meta-analysis and systematic review. ISPRS J Photogramm. Remote Sens. 2020;164:152-170.

[22] Torre DMG, Gao J, Ng MC, Shi Y. Phenology-based delineation of irrigated and rain-fed paddy fields with sentinel-2 imagery in Google earth engine. Geo Spat Inf Sci. 2021;24(4):695-710.

[23] Pan L, Xia H, Yang J, Niu W, Wang R, Song H, et al. Mapping cropping intensity in Huaihe basin using phenology algorithm, all Sentinel-2 and Landsat images in Google earth engine. Int J Appl Earth Obs Geoinf. 2021;102:102376.

[24] Kamthonkiat D, Honda K, Turral H, Tripathi N, Wuwongse V. Discrimination of irrigated and rainfed rice in a tropical agricultural system using SPOT VEGETATION NDVI and rainfall data. Int J Remote Sens. 2005;26(12):2527-2547.

[25] Landsat Missions. Landsat Collection 2 [Internet]. n.d. [cited 2022 May 1]. Available from: https://www.usgs.gov/landsat-missions/landsat-collection-2.
[26] Wang J, Xiao X, Liu L, Wu X, Qin Y, Steiner JL, et al. Mapping sugarcane plantation dynamics in Guangxi, China, by time series Sentinel-1, Sentinel-2 and Landsat images. Remote Sens Environ. 2020;247:111951.
[27] Land Development Department. [Internet]. n.d. [cited 2022 Feb 15]. Available from: https://dinonline.ldd.go.th/Login.aspx?servi ice=3.
[28] Shippert P. Digital Number, Radiance, and Reflectance [Internet]. 2013 [cited 2022 May 4]. Available from: https://www.13harrisgeospatial.com/Leaarn/Blogs/B log-Details/ArtMID/10198/ArticleID/16278/D igital-Number-Radiance-and-Reflectance.
[29] Landsat Mission. Landsat Collection 2 Quality Assessment Bands [Internet]. n.d. [cited 2022 May 4]. Available from: https://www.usgs.gov/landsat-missions/landsat-collection-2-quality-assessment-bands.
[30] Huete A, Didan K, Miura T, Rodriguez EP, Gao X, Ferreira LG. Overview of the radiometric and biophysical performance of the MODIS vegetation indices. Remote Sens Environ. 2002;83(1):195-213.
[31] Li P, Jiang L, Feng Z, Sheldon S, Xiao X. Mapping rice cropping systems using Landsat-derived renormalized index of normalized difference vegetation index (RNDVI) in the Poyang Lake Region, China. Front Earth Sci. 2016;10(2):303-314.